Published in final edited form as:
J Hazard Mater. 2019 September 05; 377: 315–320. doi:10.1016/j.jhazmat.2019.05.101.

Solution equilibria of uranyl minerals: Role of the common groundwater ions calcium and carbonate

Dovie M. Stanley[a], **Richard T. Wilkin**[b]

[a]Oak Ridge Associated Universities, U.S. Environmental Protection Agency, Office of Research and Development, National Risk Management Research Laboratory, Groundwater, Watershed, and Ecosystem Restoration Division, Ada, OK, 74820, United States

[b]U.S. Environmental Protection Agency, Office of Research and Development, National Risk Management Research Laboratory, Groundwater, Watershed, and Ecosystem Restoration Division, Ada, OK, 74820, United States

Abstract

Understanding the factors that govern aqueous solubility of uranyl minerals is important for predicting uranium mobility in groundwater and for designing effective remediation strategies. The uranyl-containing minerals metaschoepite [UO3·(2H2O)] and uranophane [Ca(UO2)2(SiO3OH)2·5H2O] were synthesized and evaluated in batch solubility experiments conducted in the presence of common groundwater ions: calcium, bicarbonate/carbonate, and dissolved silica. Solid-phase characterization revealed the expected structural and thermogravimetric properties of metaschoepite and uranophane. Metaschoepite solubility in carbonate-free water followed a u-shaped pH dependency with minimum solubility near pH 8.5; uranium concentrations at pH ≳ 8.5 were approximately equivalent to the reference value for safe drinking water established by the EPA (30 μg/L). With increasing bicarbonate/carbonate concentration (1 mM – 50 mM) the solubility of metaschoepite increased, presumably due to the formation of uranyl-carbonate complexes. However, the experimental concentrations of uranium were lower than concentrations predicted from accepted complexation constants. For uranophane, equilibrium uranium concentrations were < 75 μg/L at typical groundwater concentrations of calcium and dissolved silica (pH > 7). The diversity of uranyl minerals that possibly form in the presence of common groundwater species: Ca-Mg-Na-K-Si-bicarbonate/carbonate-sulfate-chloride, has not been fully explored with respect to understanding potential mineral transformations and impacts on uranium solubility and mobility.

Graphical abstract

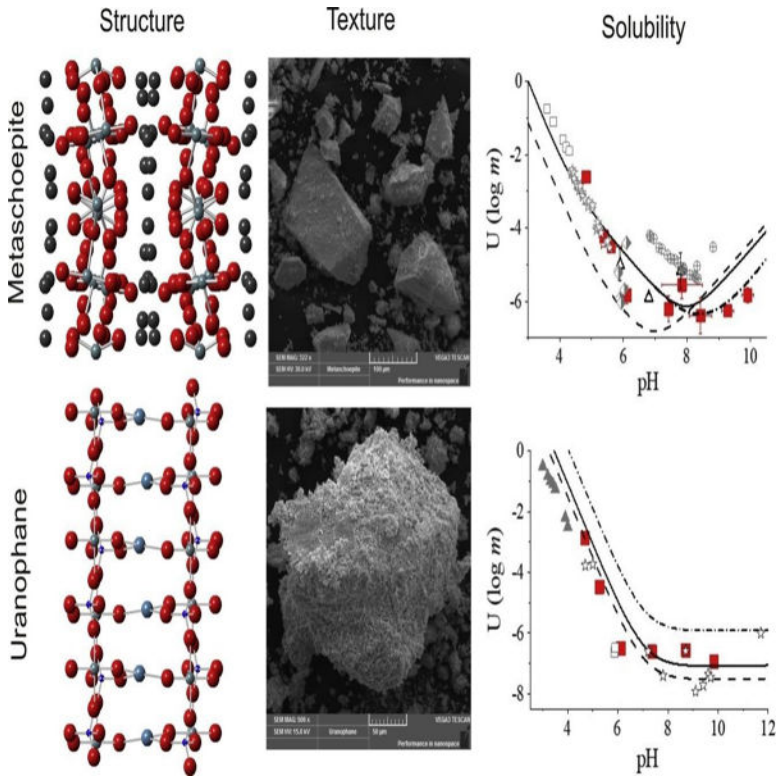

Keywords

Uranium; Groundwater; Remediation; Metaschoepite; Uranophane

1. Introduction

Uranium is a naturally occurring metal contained in bedrock and aquifer solids which can be dissolved into groundwater through water-rock interactions. Source minerals include uraninite (UO_2), coffinite ($USiO_4$), and carnotite [$K_2(UO_2)_2(VO_4)_2 \cdot 3H_2O$] (e.g., [1,2]). On regional scales, the occurrence of uranium in groundwater can be linked to geologic setting, especially the presence of granitic parent rocks and shales that serve as the primary sources of uranium-bearing minerals [3,4]. In more localized settings, uranium concentrations in groundwater can be influenced by proximity of mining and milling activities [[5], [6], [7]]. The transport and fate of uranium in groundwater environments depends on geochemical parameters such as pH, redox conditions, and the presence of ligand-forming species such as dissolved carbonate, Ca^{2+}, and Mg^{2+} ions [[8], [9], [10]]. In reducing to moderately reducing environments, crystalline U(IV) is insoluble [11]. However, when present in the U(VI) oxidation state (Eh $\gtrsim$ 350 mV at pH 7), uranium is readily soluble as the uranyl ion (UO_2^{2+}), carbonate complexes [$UO_2(CO_3)_2^{2-}$], and ternary Mg-Ca-U-CO_3 complexes, e.g., $Ca_2UO_2(CO_3)^0$, $CaUO_2(CO_3)_3^{2-}$, $Mg_2UO_2(CO_3)^0$, and $MgUO_2(CO_3)_3^{2-}$ [9,10,12]. In addition, groundwater geochemical data indicate positive correlations between uranium and nitrate, alkalinity, and calcium, suggesting possible uranium sources to groundwater through oxidative dissolution and aqueous complexation [3,13].

For naturally occurring uranium, in most cases chemical toxicity is predominant over radioactive properties for determining risk. The World Health Organization [WHO; [14]] has established a provisional guideline value for the total content of uranium in drinking water of 30 μg/L based on its chemical toxicity. The National Primary Drinking Water Regulations (NPDWR) established by the U.S. Environmental Protection Agency (U.S. EPA) also set the Maximum Contaminant Level (MCL) for uranium in drinking water at 30 μg/L. Long term exposure above the MCL may result in increased risk of cancer and kidney toxicity [15].

In situ passive remediation of oxidized U(VI) has proven to be challenging due to its high solubility, especially in the presence of complex-forming ligands [[16], [17], [18]]. Attenuation processes for U(VI) include sorption to solid surfaces present in the subsurface [19,20] and precipitation of a diverse group of uranyl minerals that depend on groundwater chemistry [21]. For example, the release of uranium (VI) from spent nuclear waste causes the formation of secondary uranium (VI) phases, such as the uranyl oxide hydrates schoepite and metaschoepite [22]. Experiments using these minerals have shown correlations between uranium solubility and the development of more complex uranyl minerals [23,24]. Subsequently, more stable and less soluble secondary phases are formed when common groundwater solutes, such as calcium and silica, are incorporated into the solid-phase interlayer spacing. Paragenetic sequences indicate that uranyl silicates can be the stable end products of the reaction sequence [22]. Thus, Na-boltwoodite [$Na(UO_2(SiO_3OH)\cdot 1.5H_2O$] and uranophane [$Ca(UO_2)_2(SiO_3OH)_2\cdot 5H_2O$] can be found around geological sites where anthropogenic activities have been documented [25]. Additionally, their thermodynamic properties have been examined to predict uranium solubility and transport in different environments [[26], [27], [28], [29], [30]].

The purpose of this study was to examine the solubility of uranyl minerals in the presence of common groundwater ions to better understand the long-term fate of uranium and possible attenuation processes in moderately oxidizing groundwater systems. In this study, we focus on the importance of calcium and inorganic carbon for influencing uranium concentrations in groundwater systems.

2. Experimental

2.1. Materials

Metaschoepite and uranophane were synthesized using methods modified from Giammar and Hering [23], Shvareva et al. [29], and Pérez et al. [26]. Reagent grade $UO_2(CH_3COO)_2\cdot 2H_2O$ (Baker), $Ca(CH_3COO)_2\cdot H_2O$ (Baker), NH_4OH (Sigma-Aldrich), $Na_2SiO_3\cdot 5H_2O$ (Sargent-Welch), and 18 mΩ water (Millipore Synergy UV-R) were used in the experimental studies. All solutions were purged with ultra-high purity N_2 gas for 1 h to remove dissolved carbon dioxide and oxygen. Metaschoepite was prepared by adding NH_4OH to 0.09 M uranyl acetate solution to bring the final pH to 8.2. Uranophane was prepared by mixing 0.09 M uranyl acetate, 0.05 M calcium acetate, and 0.09 M sodium silicate, with pH adjustment to 8.0 using NH_4OH. The yellow-colored suspensions were aged at 60 °C for 2 weeks under a N_2 atmosphere. The solids were then separated by filtration, washed with hot deionized water, and dried in a vacuum desiccator.

2.2. Characterization

Powder X-ray diffraction (XRD) patterns were obtained using a Rigaku Miniflex with Fe $K\alpha$ radiation operated at a voltage of 30 kV. Thermogravimetric analyses (TGA) were performed using a Netzsch STA409 TGA/DSC coupled to a Pfeiffer GSD301 mass spectrometer (MS). Samples were placed in Pt crucibles and heated to 1000 °C at a rate of 10 °C/min under argon gas flow of 50 mL/min. The off-gases, carbon dioxide and water, were monitored at mass-to-charge ratios (m/z) of 44 (CO_2^+) and 18 (H_2O^+), respectively. A TESCAN Vega3 scanning electron microscope (SEM) with an Element energy dispersive spectrometer was used to examine particle morphology and elemental composition. Quality control analyses for the XRD and TGA-MS measurements utilized NIST 640b standard reference material (silicon powder) and calcium carbonate (Sigma-Aldrich, 99.999%), respectively.

2.3. Solubility studies

Batch solubility experiments were setup by adding 20–120 mg of synthetic uranyl minerals to triplicate 45-mL vials with rubber septum lids. Buffer solutions (pH 4–10; 5 mM KHP, potassium hydrogen phthalate; 5 mM MES, 2-(N-morpholino)ethanesulfonic acid; 5 mM HEPES, 4-(2-hydroxyethyl)-1-piperazineethanesulfonic acid; 6 mM NH_4Cl-NH_4OH; and 16 mM NH_4OH) were prepared using N_2-purged water. Ammonium was used as the preferred solution cation to minimize the possibility of secondary phase formation during the solubility experiments [21]. The vials were equilibrated in a water bath (Thermo MaxQ7000) set at 25 °C for up to 60 days. Samples were monitored using a pH meter and electrode (Orion semi-micro) calibrated with NIST-traceable buffers (4.01, 7.00, and 10.00). Filtered solutions (0.22-μm) were acidified (pH < 2; Optima HNO_3) and analyzed using inductively coupled plasma – optical emission spectrometry (ICP-OES, Perkin Elmer Optima 8300DV; analysis based on EPA Method 200.7). For lower detection levels (<100 μg/L), magnetic sector mass spectrometry using medium resolution mode was used for a quantitation level of 1 μg/L (R = 4000; HR-ICP-MS; Thermo Scientific Element XR; analysis based on EPA Method 200.8). Quality control samples included lab duplicates, blanks, matrix spikes, calibration check standards, and second-source quality control samples (see Supplementary data).

Additional solubility studies at 25 °C were established using uranyl minerals and additions of solid $CaCO_3$ (Sigma-Aldrich), dissolved Si (from $Na_2SiO_3{\cdot}5H_2O$), dissolved Ca (from $Ca(NO_3)_2$; Baker), and dissolved inorganic carbon (from $NaHCO_3$; Baker). The aqueous activities of U(VI) species were calculated using Geochemist's Workbench software package (v. 8, Aqueous Solutions LLC) and thermodynamic data from Guillaumont et al. [30]. Activity coefficients were determined using the Debye-Hückel equation [31],

$$\log\gamma_i = -\frac{Az_i^2\sqrt{I}}{1 + a_iB\sqrt{I}} \quad (1)$$

where γ_i is the activity coefficient of an ion with electrical charge z_i, I is the solution ionic strength, A and B are temperature-dependent constants, and a_i is the effective diameter.

3. Results and discussion

3.1. Characterization of synthetic solids

Powder X-ray diffraction patterns collected for the synthetic solids showed d-space patterns consistent with schoepite/metaschoepite and uranophane (Fig. 1a). Thermogravimetric measurements confirmed the stoichiometric formula of water in each sample (Fig. 1b). The TGA curves show multiple steps of mass loss, which correspond to the calorimetric results and TGA-MS off-gas profiles (Fig. 1c–d). For schoepite/metaschoepite, the 416–516 °C temperature range was used for the calculation of water content (11.25 ± 0.05 wt%), yielding 1.96 mol of water per formula unit, consistent with the expected composition of metaschoepite ($UO_3 \cdot 2H_2O$). For uranophane, the second mass loss step from 550 to 650 °C was used which yielded the expected 5.2 mol of water per formula unit.

Stacked DSC thermograms showed up to four transitions for the synthetic materials that correspond to the removal of water (Fig. 1c). Metaschoepite showed three endotherms at 93, 136, and 274 °C, respectively, and an exotherm at 405 °C. These transitions represent the partial removal of interlayer water and decomposition of uranyl-hydroxyl complex into uranium trioxide, respectively. Uranophane showed two endothermic transitions and one small exothermic transition at 94, 142, and 722 °C, respectively. For uranophane, the endotherms are due to water evolution [32,33] and the exotherm transition is probably due to hydroxyl reduction from silicate molecules since no peak is seen in the evolved gas profile for the mineral decomposition product, water, at m/z 18 (Fig. 1d). The synthetic metaschoepite and uranophane powders were fine-grained and readily dispersed into the buffer solutions to facilitate dissolution reactions.

3.2. Metaschoepite solubility analysis

Metaschoepite solubility measurements at variable pH conditions were performed to establish a baseline for comparison to experiments conducted with calcium and bicarbonate/carbonate additions. Over the pH range from about 4 to 10, uranium concentrations stabilized within seven days, but sample collection extended out to ~58 days to confirm steady-state solubility trends (Fig. S1 and Fig. S2). All solubility values were established from undersaturated conditions. The experimental pH-dependent solubility profile for metaschoepite indicated a minimum solubility at pH ~8.5 (Fig. 2). At pH < 7, the measured solubility points generally fell in between the trends predicted by the metaschoepite solubility models of Guillaumont et al. [30] and Langmuir [34], except at pH < 5 where a higher uranyl solubility was measured compared to model predictions (Fig. 2). Previous solubility data from Sandino and Bruno [35], Kramer-Schnabel et al. [36], Gorman-Lewis et al. [37], Giammar and Hering [23], and Jang et al. [38] are plotted for comparison (Fig. 2). At pH > 8, the measured solubility of metaschoepite was lower but along the same increasing trend as predicted by the Guillaumont et al. [30] and Langmuir [34] models. An improved fit was obtained by adjusting the equilibrium constant (log K) of the reaction:

$$UO_2^{2+} + 3H_2O \rightleftharpoons UO_2(OH)_3^- + 3H^+ \quad (2)$$

from −20.25 to −23 (Fig. 2; adjusted trend). The high pH (>8) experimental data are significant because they represent the lowest measured solubility values for metaschoepite to date and the solubility data presented here provide a wider pH scan for metaschoepite in comparison to previous studies.

At saturation with metaschoepite, uranium aqueous species are predicted to be mainly polymeric species across the pH range studied here (Fig. S3). At low pH (<5), the dominant solubility-controlling reaction is expected to be:

$$2UO_3 \cdot 2H_2O_{(s)} + 2H^+ \rightleftharpoons (UO_2)_2(OH)_2^{2+} + 2H_2O \quad (3)$$

At near-neutral pH ($5 \lesssim pH \lesssim 8$), the solubility controlling reaction is expected to be:

$$3UO_3 \cdot 2H_2O_{(s)} + H^+ \rightleftharpoons (UO_2)_3(OH)_5^+ \quad (4)$$

At moderately alkaline conditions ($8 \lesssim pH \lesssim 10$), the solubility controlling reaction is expected to be controlled by the monomeric species, $UO_2(OH)_3^-$:

$$UO_3 \cdot 2H_2O_{(s)} \rightleftharpoons UO_2(OH)_3^- + H^+ \quad (5)$$

The experimental data plotted in Fig. 2 represent uncorrected concentration data from the experiments that were conducted at low ionic strength (≲0.025 m). The model predictions, on the other hand, represent predicted species activities or thermodynamic concentrations. As the ionic strength approaches 0 (infinite dilution), differences between mass-based and thermodynamic concentrations become negligible, especially when compared on a logarithmic scale (Fig. 2).

In this study, we minimized the possibility of secondary phase formation during the metaschoepite solubility tests by avoiding the use of sodium- and/or calcium-bearing salts in the buffer solutions [21]. The measured solubility points at pH ˜6 and ˜8 are similar to previous data from the literature but are incongruous with other measured points in this study (Fig. 2). The reason(s) for this is not clear but may be related to pH-specific aging and solid-phase transformation processes that were not explored in detail as part of this study. For the purposes of determining geochemical conditions favorable for U(VI) attenuation in groundwater, it is notable that at the solubility minimum, the measured uranium concentration in equilibrium with metaschoepite was ˜$10^{-6.73}$ M (44 μg/L), or approximately equivalent to the reference value for safe water established by the EPA (30 μg/L; [15]).

With increasing bicarbonate/carbonate concentration the solubility of metaschoepite increased, presumably due to the formation of uranyl-carbonate complexes (Fig. 3). In all cases, the experimental concentrations of uranium were lower than concentrations predicted by using the generally accepted complexation constants from Guillaumont et al. [30]. Agreement between the experimentally determined and modelled uranium concentrations improved at higher pH and higher bicarbonate/carbonate levels (up to 50 mM; ±30%). Poor

agreement was apparent at bicarbonate/carbonate concentrations near 1 mM, although even at these low concentrations of dissolved inorganic carbon, uranium concentrations were elevated relative to inorganic carbon-free systems. It is possible that at the lower levels of added bicarbonate/carbonate other reactions (e.g., surface adsorption) lowered the concentration of available complexing species and thus led to the lower than expected uranium concentrations in solution shown in Fig. 3.

3.3. Uranophane solubility analysis

Uranophane solubility experiments reported on here differed from previous experiments in two ways. First, the duration of experiments in this study was thirty days; previous studies used 7 days as the equilibration period. However, we also observed non-changing concentrations after about 7 days (Fig. S4). Secondly, buffers were used at pH ˜4.5 and ˜8.5 to maintain fixed pH conditions. In all experiments, pH remained in control with a standard deviation of ˜0.1 standard units. The experimental uranium concentrations reasonably followed the uranophane solubility models of Chen et al. [39], Nguyen et al. [40], and Langmuir [34] (Fig. 4). In the slightly acidic range (pH 4 to 6), experimental samples were less soluble than the model predictions (Fig. 4). Uranophane solubility measurements were also consistent with previous data from Casas et al. [41], Prikryl [42], and Shvareva et al. [29]. Note uranophane solubility tests by Pérez et al. [26] were conducted in the presence of dissolved inorganic carbon; consequently, uranium concentrations were elevated in their system compared to systems free of bicarbonate/carbonate (Fig. 4, Fig. S4).

At near-neutral pH, the solubility controlling reaction for uranophane is expected to be:

$$\begin{aligned} &Ca(UO_2)_2(SiO_3OH)_2 \cdot 5H_2O + 2H^+ \\ &\rightleftharpoons Ca^{2+} + 2H_4SiO_{4(aq)} + 2UO_2(OH)_{2(aq)} + H_2O \end{aligned} \quad (6)$$

Thus, at constant pH the equilibrium U(VI) concentration is expected to decrease with increasing dissolved calcium and/or dissolved silica. The theoretical solubility curves in Fig. 4 reflect a calcium ion concentration of 1.2 mM (48 mg/L) and a silicon concentration of 0.9 mM (25 mg/L). These concentrations for calcium and silicon are reasonable for groundwater systems. Calcium concentrations in groundwater are in the range from about 0.2 mM to 25 mM and silicon concentrations typically fall in between the solubilities of quartz and amorphous silica (˜0.2 mM to ˜1 mM; [43]). The total ionic strength ranged from about 10 to 25 mM, a range consistent with natural groundwater systems. Uranyl ion solubility was reduced by the presence of higher concentrations of either or both of these solution components. This reduction in solubility seems to be due to the common ion effect. Equilibrium uranium concentrations at pH > 7 were <75 μg/L (Fig. 4). By increasing the concentrations of calcium and/or dissolved silica, the effect of stabilizing uranophane and driving down the concentration of U(VI) species is expected. The results from Pérez et al. [26], however, demonstrate the important influence of uranyl-carbonate complexation on increasing uranium concentrations and facilitating migration in groundwater.

3.4. Calcite buffering in the solid-phase

To further examine uranium solubility in the presence of calcium and bicarbonate/carbonate ions, experiments were conducted with metaschoepite plus calcite in the solid-phase and with increasing addition of calcium ions in solution at pH 8.5. These experiments were intended to mimic slightly alkaline aquifer systems saturated with calcium carbonate. With dissolved calcium additions of 10 and 100 mg/L, respectively, uranium concentrations were significantly elevated (up to 50×) compared to the baseline metaschoepite solubility at pH 8.5 without calcium and bicarbonate/carbonate ions available for complexation (Fig. 5). These data demonstrate the impact that calcium and inorganic carbon ions have on the mobility of U(VI) and are consistent with the formation of ternary Ca-U−CO_3 complexes, e.g., $Ca_2UO_2(CO_3)^0$ and $CaUO_2(CO_3)_3^{2-}$ [7,9].

However, with increasing calcium ion addition, the observed solubility of uranium decreased (Fig. 5). This behavior suggests uranium removal in the presence of calcite at elevated calcium concentrations (>2.5 mM). The increase in calcium ion concentration at pH 8.5 is expected to remove excess bicarbonate/carbonate through calcium carbonate precipitation; consequently, the impact of uranyl-carbonate complexation is minimized. The extent of uranium retention is expected to increase with the loss of uranium-calcium-carbonate complexes [44]. In the presence of calcite and dissolved calcium, metaschoepite was possibly transformed to becquerelite $Ca[(UO_2)_6O_4(OH)_6]$. Inorganic carbon concentrations were determined to be 0.18, 0.16, and 0.032 mM for the 10, 100, 500 mg/L calcium ion addition experiments, respectively. Geochemical models indicated that the solution composition ranged from saturated to under-saturated with respect to becquerelite (Table S1). Thus, it is possible that a more stable phase with lower solubility than becquerelite formed from metaschoepite plus calcite in solution containing calcium ions. Additional studies are needed to better understand the mechanisms responsible for uranium removal in systems containing solid-phase carbonate.

3.5. Implications for uranium attenuation in groundwater

The experimental results further establish that in moderately oxidizing groundwater at pH < 6 and with low to high levels of dissolved inorganic carbon, U(VI) species are soluble and potentially mobile. The experimental findings also show, however, that at moderately alkaline conditions (pH ~ 8.5) uranium retention in the solid-phase is expected to increase with the loss of complexing potential of inorganic carbon and calcium. Modeling studies of metaschoepite and uranophane solubility over a range of pH (5–8), PCO_2 (0.001 to 0.1), Si (0.035 to 0.35 mM), and fixed Ca (1 mM) indicated that the lowest U(VI) concentrations achievable (10^{-7} to 10^{-6} M) were at higher levels of dissolved silica, low PCO_2, and pH 6–7 (Fig. S5, S6). Thus, there are potential geochemical manipulations for aquifer systems that could enhance natural attenuation processes, especially for systems at near-neutral to slightly alkaline pH. There remains complexity and uncertainty regarding the transformations of uranyl-containing minerals and potential stabilization effects, but these mineral transformation processes could enhance natural attenuation of uranium [45].

4. Conclusions

This study examined groundwater conditions that could be favorable for the attenuation of U(VI) contamination. Precipitation of metaschoepite and/or uranophane at near-neutral pH to moderately alkaline conditions can result in uranium concentrations that are just above safe drinking water thresholds. Low pH (pH < 6) and PCO_2 levels >0.01 favor uranium mobility. Whereas, near-neutral to moderately alkaline pH, low PCO_2 (˜0.001), and elevated silica concentrations are more favorable for U(VI) attenuation. The diversity of uranyl minerals that possibly form in the presence of common groundwater species: Ca-Mg-Na-K-Si-bicarbonate/carbonate-sulfate-chloride, has not been fully explored with respect to understanding mineral transformations and impacts on soluble uranium concentrations. At moderately alkaline groundwater conditions, the presence of solid-phase carbonate and excess calcium concentrations are beneficial for removing uranyl species due to the minimization of uranyl-calcium-carbonate complexes. Additional studies are needed to better understand the geochemical fate of uranium in the presence of common groundwater cations and anions.

Supplementary Material

Refer to Web version on PubMed Central for supplementary material.

Acknowledgement

The EPA through its Office of Research and Development funded and conducted this research. The views expressed in this paper are those of the authors and do not necessarily reflect the views or policies of EPA. Mention of trade names or commercial products does not constitute endorsement or recommendation for use. We thank Ms. Kim Schuerger for assistance with the TGA-MS measurements.

References

1. Stalder E, Blanc A, Haldimann M, Dudler V. Occurrence of uranium in Swiss drinking water Chemosphere, 86 (2012), pp. 672–679 [PubMed: 22154002]
2. Ranalli AJ, Yager DB Use of mineral/solution equilibrium calculations to assess the potential for carnotite precipitation from groundwater in the Texas Panhandle, USA Appl. Geochem, 73 (2016), pp. 118–131
3. Banning N. Pawletko J. Röder C. Kübeck F. Wisotzky Ex situ groundwater treatment triggering the mobilization of geogenic uranium from aquifer sediments Sci. Total Environ, 587 (2017), pp. 371–380 [PubMed: 28237470]
4. Post V, Vassolo S, Tiberghien C, Baranyikwa D, Miburo D. Weathering and evaporation controls on dissolved uranium concentrations in groundwater–A case study from northern Burundi Sci. Total Environ, 607 (2017), pp. 281–293 [PubMed: 28692898]
5. Abdelouas W. Lutze E. Nuttall Chemical reactions of uranium in ground water at a mill tailings site J. Contam. Hydrol, 34 (1998), pp. 343–361
6. Gómez P, Garralón A, Buil B, Turrero MJ, Sánchez L, De B. Modeling of geochemical processes related to uranium mobilization in the groundwater of a uranium mine Sci. Total Environ, 366 (2006), pp. 295–309 [PubMed: 16198395]
7. Saunders JA, Pivetz BE, Voorhies N, Wilkin RT Potential aquifer vulnerability in regions down-gradient from uranium in situ recovery (ISR) sites J. Environ. Manage, 183 (2016), pp. 67–83 [PubMed: 27576149]
8. Giblin B. Batts D. Swaine Laboratory simulation studies of uranium mobility in natural waters Geochim. Cosmochim. Acta, 45 (1981), pp. 699–709

9. Bernhard G, Geipel G, Brendler V, Nitsche H. Speciation of uranium in seepage waters of a mine tailing pile studied by time-resolved laser-induced fluorescence spectroscopy (TRLFS) Radiochim. Acta, 74 (1996), pp. 87–92
10. Lee J-Y, Vespa M, Gaona X, Dardenne K, Rothe J, Rabung T, Altmaier M, Yun J-I Formation, stability and structural characterization of ternary MgUO2(CO3)3 2− and Mg2UO2(CO3)3 (aq) complexes Radiochim. Acta, 105 (2017), pp. 171–185
11. Seder-Colomina M, Mangeret A, Stetten L, Merrot P, Diez O, Julien A, Barker E, Thouvenot A, Bargar J, Cazala C, Morin G. Carbonate facilitated mobilization of uranium from lacustrine sediments under anoxic conditions Environ. Sci. Technol, 52 (2018), pp. 9615–9624 [PubMed: 29983058]
12. Prat O, Vercouter T, Ansoborlo E, Fichet P, Perret P, Kurttio P, Salonen L. Uranium speciation in drinking water from drilled wells in southern Finland and its potential links to health effects Environ. Sci. Technol, 43 (2009), pp. 3941–3946 [PubMed: 19544911]
13. Nolan J, Weber KA Natural uranium contamination in major US aquifers linked to nitrate Environ. Sci. Technol. Lett, 2 (2015), pp. 215–220
14. World Health Organization Guidelines for Drinking Water Quality (4th ed), World Health Organization, Geneva, Switzerland (2011)
15. US Environmental Protection Agency National Primary Drinking Water Regulations, in (2018) accessed 25 September https://www.epa.gov/ground-water-and-drinking-water/national-primary-drinking-water-regulations
16. Lammers LN, Rasmussen H, Adilman D, Zeeb P, Larson DG, Quicksall AN Groundwater uranium stabilization by a metastable hydroxyapatite Appl. Geochem, 84 (2017), pp. 105–113
17. Emerson HP, Di Pietro S, Katsenovich Y, Szecsody J. Potential for U sequestration with select minerals and sediments via base treatment J. Environ. Manage, 223 (2018), pp. 108–114 [PubMed: 29908396]
18. Lu S, Zhu K, Hayat T, Alharbi NS, Chen C, Song G, Chen D, Sun Y. Influence of carbonate on sequestration of U(VI) on perovskite J. Hazard. Mater, 364 (2019), pp. 100–107 [PubMed: 30342289]
19. Catalano JG, Brown GE Jr Uranyl adsorption onto montmorillonite: evaluation of binding sites and carbonate complexation Geochim. Cosmochim. Acta, 69 (2005), pp. 2995–3005
20. Jemison NE, Johnson T, Shiel A, Lundstrom C. Uranium isotopic fractionation induced by U(VI) adsorption onto common aquifer minerals Environ. Sci. Technol, 50 (2016), pp. 12232–12240 [PubMed: 27758097]
21. Finch R, Murakami T. Systematics and paragenesis of uranium minerals Rev. Mineral. Geochem, 38 (1999), pp. 91–180
22. Wronkiewicz DJ, Bates JK, Wolf SF, Buck EC Ten-year results from unsaturated drip tests with UO2 at 90 °C: implications for the corrosion of spent nuclear fuel J. Nucl. Mater, 238 (1996), pp. 78–95
23. Giammar DE, Hering JG Influence of dissolved sodium and cesium on uranyl oxide hydrate solubility Environ. Sci. Technol, 38 (2004), pp. 171–179 [PubMed: 14740733]
24. Plášil J. Uranyl-oxide hydroxy-hydrate minerals: their structural complexity and evolution trends Eur. J. Mineral., 30 (2018), pp. 237–251
25. Fayek M, Ren M. Paragenesis and Geochronology of the Nopal I Uranium Deposit, Mexico, in Yucca Mountain Project, Las Vegas, Nevada (2007)
26. Pérez I, Casas I, Martín M, Bruno J. The thermodynamics and kinetics of uranophane dissolution in bicarbonate test solutions Geochim. Cosmochim. Acta, 64 (2000), pp. 603–608
27. Ilton ES, Liu C, Yantasee W, Wang Z, Moore DA, Felmy AR, Zachara JM The dissolution of synthetic Na-boltwoodite in sodium carbonate solutions Geochim. Cosmochim. Acta, 70 (2006), pp. 4836–4849
28. Gorman-Lewis D, Mazeina L, Fein JB, Szymanowski JE, Burns PC, Navrotsky A. Thermodynamic properties of soddyite from solubility and calorimetry measurements J. Chem. Thermodyn, 39 (2007), pp. 568–575

29. Shvareva TY, Mazeina L, Gorman-Lewis D, Burns PC, Szymanowski JE, Fein JB, Navrotsky A. Thermodynamic characterization of boltwoodite and uranophane: enthalpy of formation and aqueous solubility Geochim. Cosmochim. Acta, 75 (2011), pp. 5269–5282
30. Guillaumont R, Fanghanel T, Fuger J, Grenthe I, Neck V, Palmer DA, Rand MH Chemical Thermodynamics 5, Update on the Chemical Thermodynamics of Uranium, Neptunium, Plutonium, Americium and Technetium, Nuclear Energy Agency OECD, Elsevier, Amsterdam (2003)
31. Stumm W, Morgan JJ Aquatic Chemistry: An Introduction Emphasizing Chemical Equilibria in Natural Waters (2nd ed.), Wiley Interscience, New York, NY (1981)
32. Urbanec Z, Mrázek Z, Čejka J. Thermal and infrared spectrum analyses of some uranyl silicate minerals Thermochim. Acta, 93 (1985), pp. 525–528
33. Chernorukov N, Kortikov V. Na[HSiUO6]·H2O: synthesis, structure, and properties Radiochemistry, 43 (2001), pp. 229–232
34. Langmuir D. Aqueous Environmental Geochemistry Prentice Hall (1997)
35. Sandino A, Bruno J. The solubility of (UO2)3(PO4)2·4H2O(s) and the formation of U(VI) phosphate complexes: their influence in uranium speciation in natural waters Geochim. Cosmochim. Acta, 56 (1992), pp. 4135–4145
36. Kramer-Schnabel U, Bischoff H, Xi R, Marx G. Solubility products and complex formation equilibria in the systems uranyl hydroxide and uranyl carbonate at 25 °C and I= 0.1 M Radiochim. Acta, 56 (1992), pp. 183–188
37. Gorman-Lewis D, Burns PC, Fein JB Review of uranyl mineral solubility measurements J. Chem. Thermodyn, 40 (2008), pp. 335–352
38. Jang J-H, Dempsey BA, Burgos WD Solubility of schoepite: comparison and selection of complexation constants for U(VI) Water Res., 40 (2006), pp. 2738–2746 [PubMed: 16780919]
39. Chen F, Ewing RC, Clark SB The Gibbs free energies and enthalpies of formation of U6+ phases: an empirical method of prediction Am. Mineral, 84 (1999), pp. 650–664
40. Nguyen SN, Silva RJ, Weed HC, Andrews JE Jr Standard Gibbs free energies of formation at the temperature 303.15 K of four uranyl silicates: soddyite, uranophane, sodium boltwoodite, and sodium weeksite J. Chem. Thermodyn, 24 (1992), pp. 359–376
41. Casas I, Pérez I, Torrero E, Bruno J, Cera E, Duro L. Dissolution Studies of Synthetic Soddyite and Uranophane, in Swedish Nuclear Fuel and Waste Management Co. (1997)
42. Prikryl JD Uranophane dissolution and growth in CaCl2–SiO2 (aq) test solutions Geochim. Cosmochim. Acta, 72 (2008), pp. 4508–4520
43. Rimstidt JD, Barnes H. The kinetics of silica-water reactions Geochim. Cosmochim. Acta, 44 (1980), pp. 1683–1699
44. Stewart BD, Mayes MA, Fendorf S. Impact of uranyl−calcium−carbonato complexes on uranium (VI) adsorption to synthetic and natural sediments Environ. Sci. Technol, 44 (2010), pp. 928–934 [PubMed: 20058915]
45. Ford RG, Wilkin RT Monitored Natural Attenuation of Inorganic Contaminants in Ground Water, in: Assessment for Radionuclides Including Tritium, Radon, Strontium, Technetium, Uranium, Iodine, Radium, Thorium, Cesium, and Plutonium-americium US Environmental Protection Agency, EPA/600/R-10/093, Washighton, DC (2010)

Highlights

- Metaschoepite yields low U(VI) concentrations in CO_2-poor groundwater at near-neutral pH.
- Uranophane produces low U(VI) concentrations at typical groundwater concentrations of calcium and silica.
- PCO_2>0.01 and pH < 6 favor U(VI) mobility.
- U(VI) attenuation is favored at near-neutral pH and when PCO_2 is minimized.

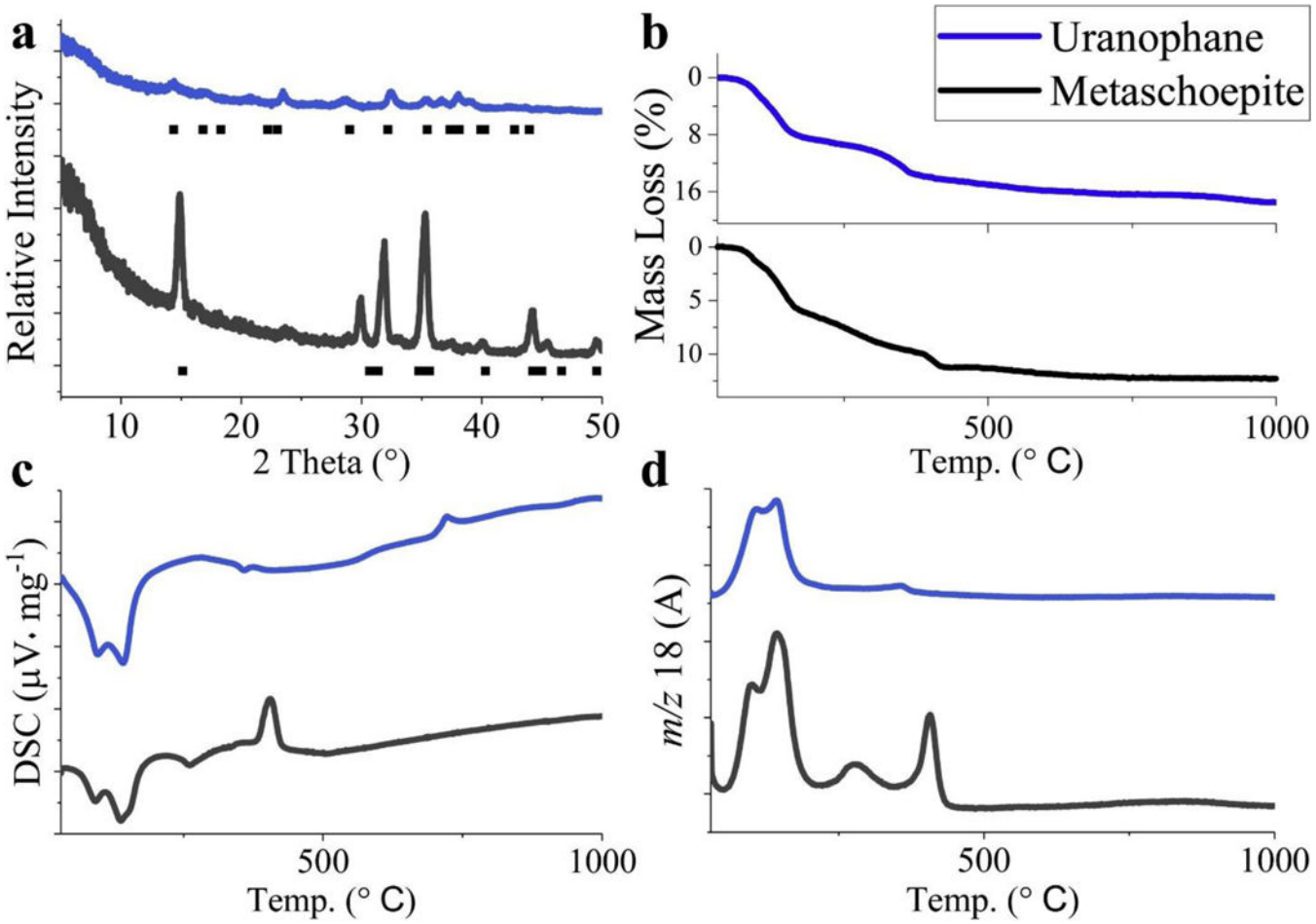

Fig. 1.

Material characterization of metaschoepite and uranophane. (a) Stacked diffractograms and peak positions from published data (metaschoepite Powder Diffraction File 43-0364; uranophane RRUFF ID R060962.9). (b) Stacked thermograms using DSC-TGA-MS for gravimetric measurements to calculate water content, (c) calorimetric DSC results showing thermal stability up to 1000 °C, and (d) gas profiles of water at mass-to-charge *(m/z)* 18 from material decomposition.

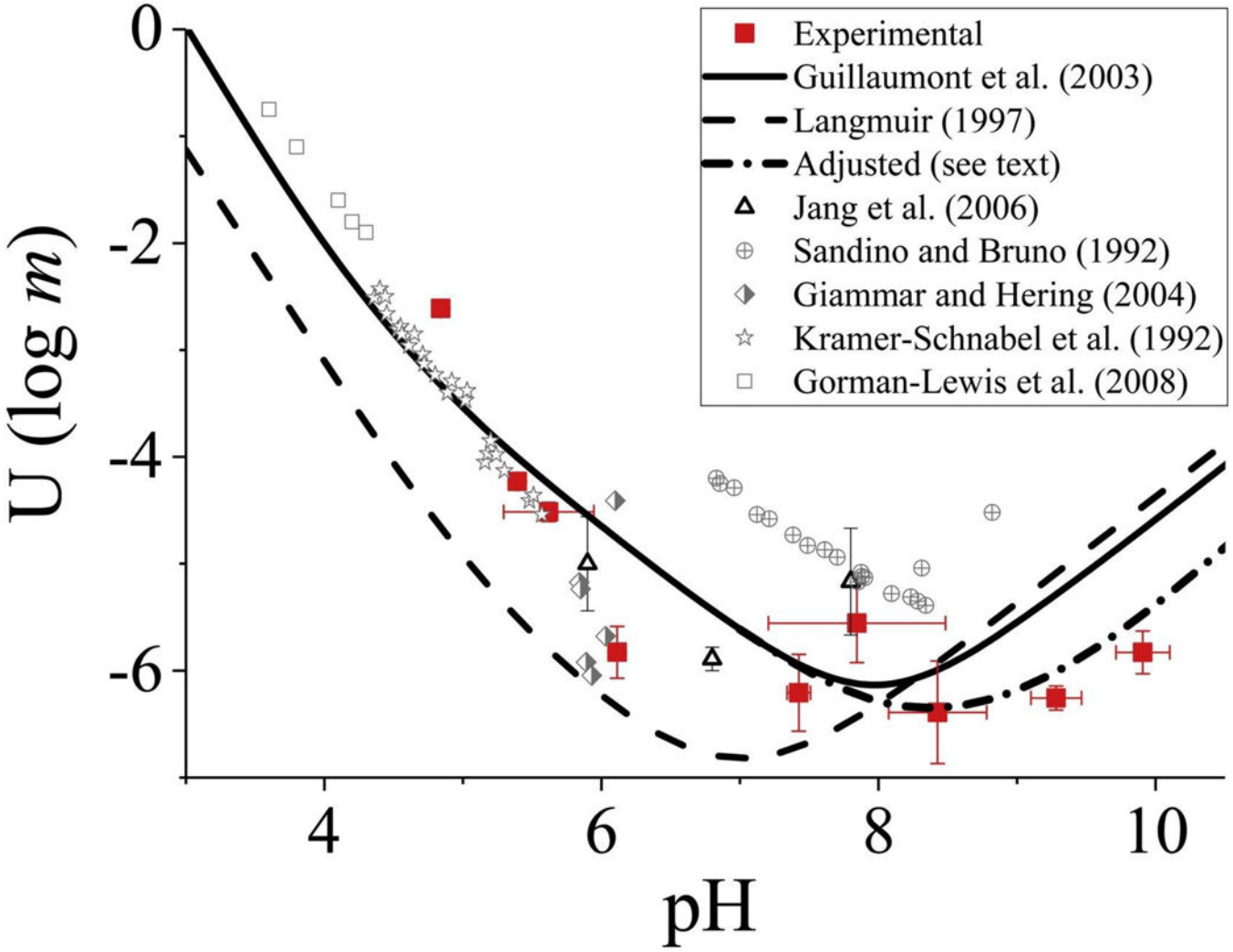

Fig. 2.

Uranium solubility diagram for metaschoepite with theoretical curves (lines) and experimental measurements (symbols; experimental data from this study are shown with red squares) as log molality of U versus pH [data sources: 23, 30, 34–38]. Uncertainty is based on pH and U concentration data collected over 58 days (Table S2) (For interpretation of the references to colour in this figure legend, the reader is referred to the web version of this article.).

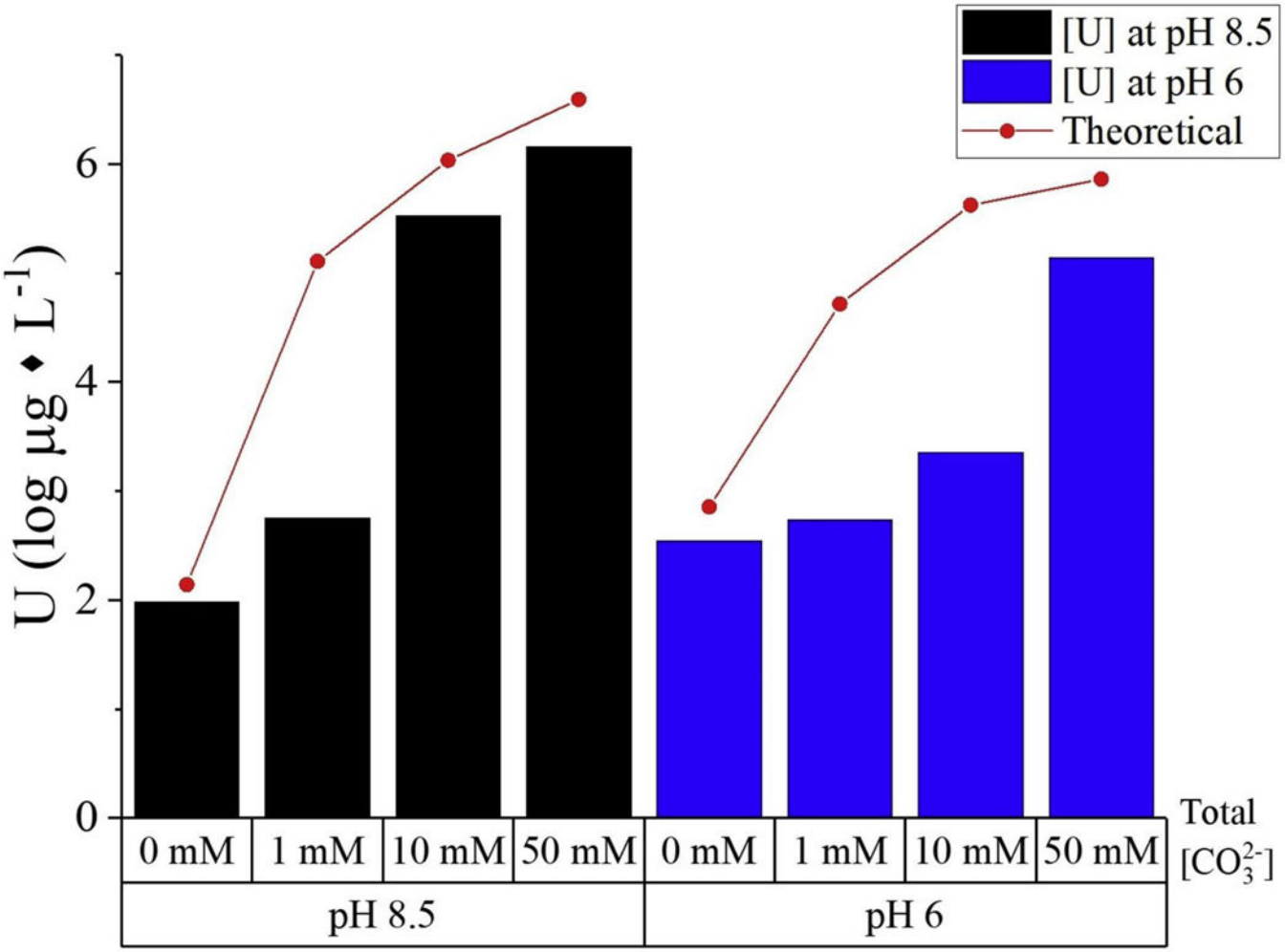

Fig. 3.

Experimental measurements of uranium solubility as log (μg L^{-1}) against sodium bicarbonate concentration at 0, 1, 10, 50 mM for metaschoepite after 14 days. The experimental results are compared to theoretical predictions using thermodynamic data from ref [30].

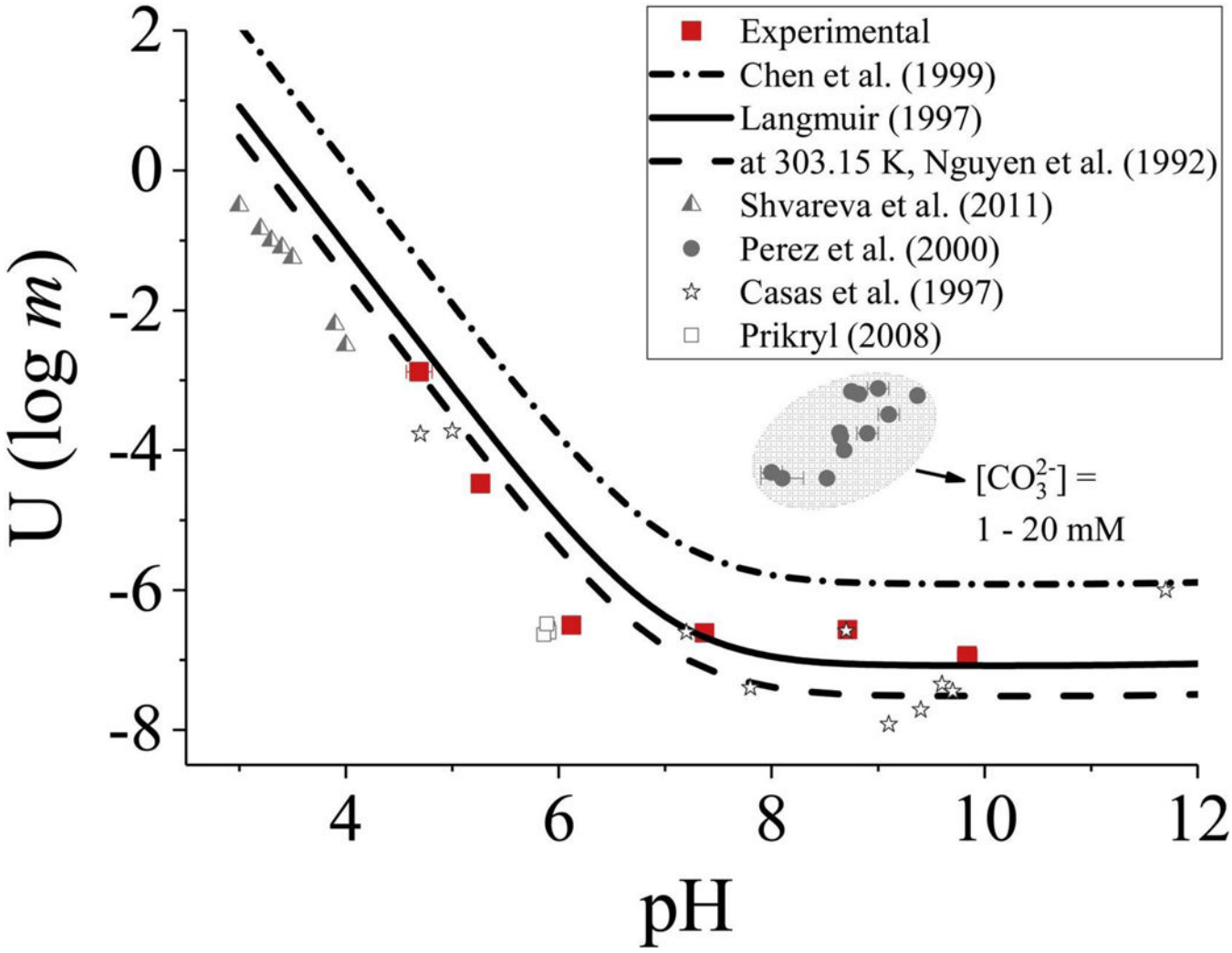

Fig. 4.

Plot of theoretical and experimental measurements of uranium solubility as log molality against pH for uranophane (symbols; experimental data from this study are shown with red squares) [data sources: [29, 34, [39], [40], [41], [42]] (For interpretation of the references to colour in this figure legend, the reader is referred to the web version of this article.).

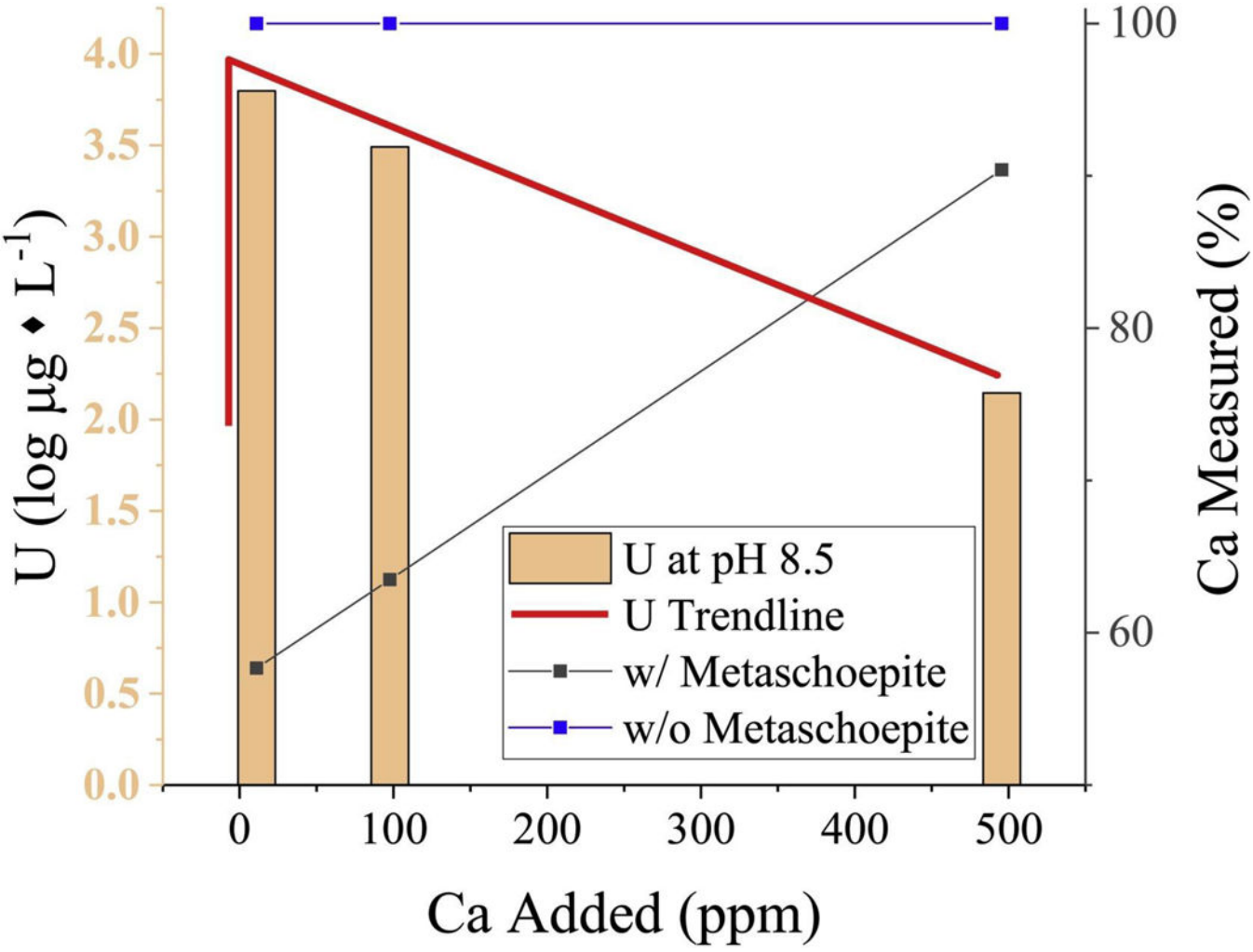

Fig. 5.

Plot of experimental measurements of uranium solubility as log (µg * L^{-1}) in systems with metaschoepite plus calcite and additions of soluble calcium ions (pH 8.5). The aging time was 35 days.